INTRACELLULAR PERMEATION OF Na^+ IN AN ACTIVE STATE GPROTEIN COUPLED RECEPTOR

SUPPLEMENTAL INFORMATION

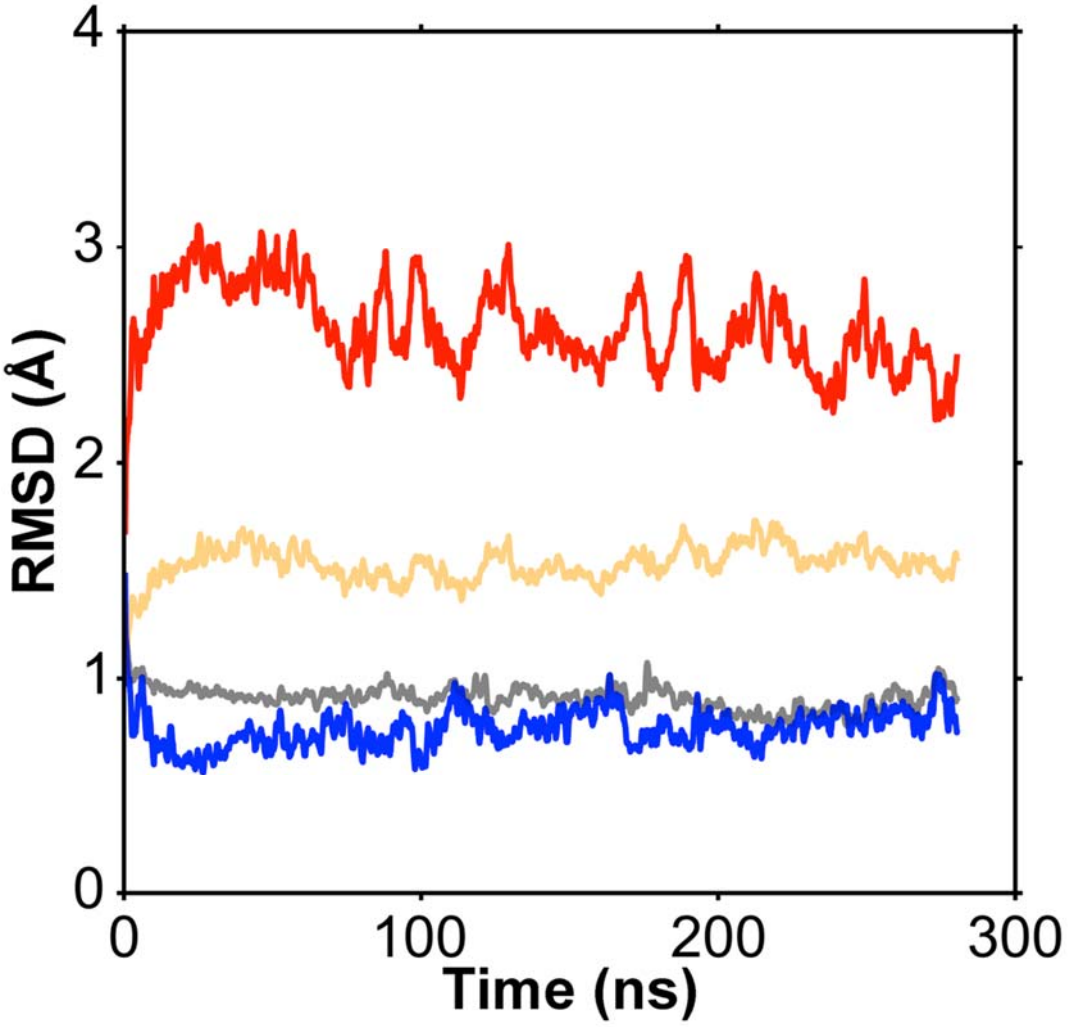

Figure S1: Backbone RMSD values during a targeted MD simulation from the inactive to the active state of m2r.

The red and blue lines correspond to the RMSD of helix TM6 relative to the inactive and active state structures (PDB: 3UON, 4MQT), respectively. The grey and orange lines correspond to the RMSD of all transmembrane helices relative to the inactive and active state structures, respectively. The RMSD of TM6 with respect to the active state structure remains below 1Å following the transition (blue line: TM6 vs. active). The RMSDs of all seven TM helices were calculated using the backbone atoms of residues 25-46, 60-83, 96-123, 140-158, 189-210, 388-408, 422-443; those of TM6 - from the residues 388-408.

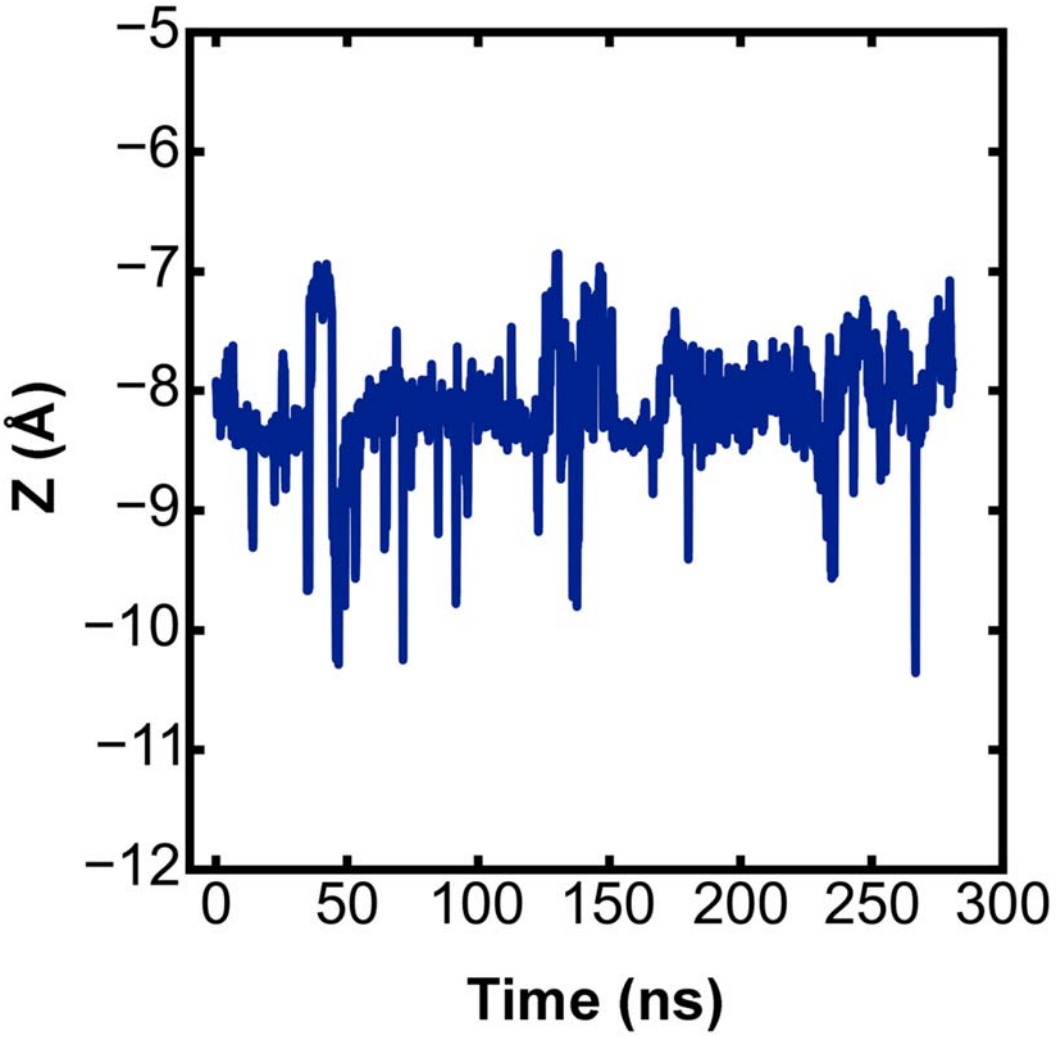

Figure S2: Position of Na^+ during a targeted MD simulation from the inactive to the active state of m2r.

The position of the Na^+ ion remains stable throughout the transition of the m2r from the inactive to active conformation. The position is reported relative to the $D103^{3.32}$ Cα atom in the orthosteric ligand binding pocket.

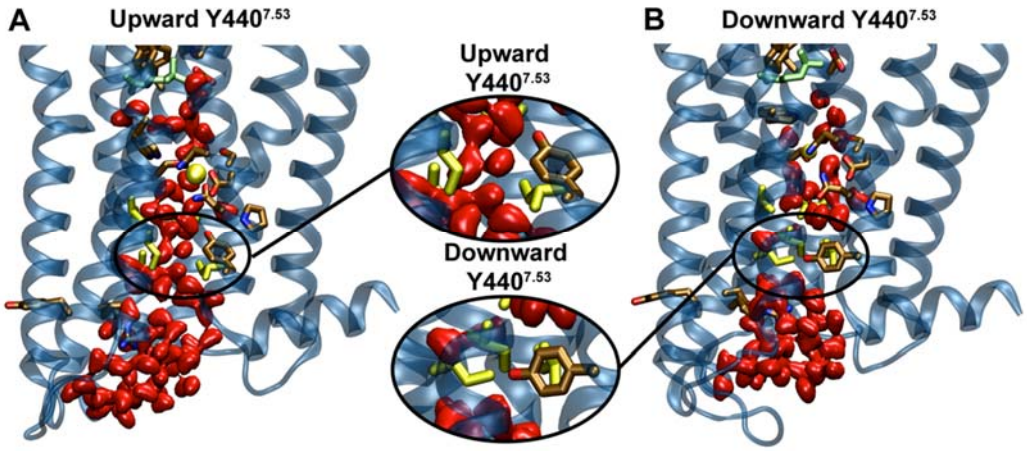

Figure S3: Y440$^{7.53}$ conformations used in pK_a and PMF calculations.

Representative frames corresponding to the most populated states of the Y440$^{7.53}$ sidechain, showing it in an upward **(A)** and downward conformation **(B)**. Water molecules are shown in red surface representation, the allosteric Na^+ ion is depicted as a yellow sphere, and the residues comprising the hydrophobic layer are displayed as yellow sticks. The bound ligand carbachol is shown in light green stick representation.

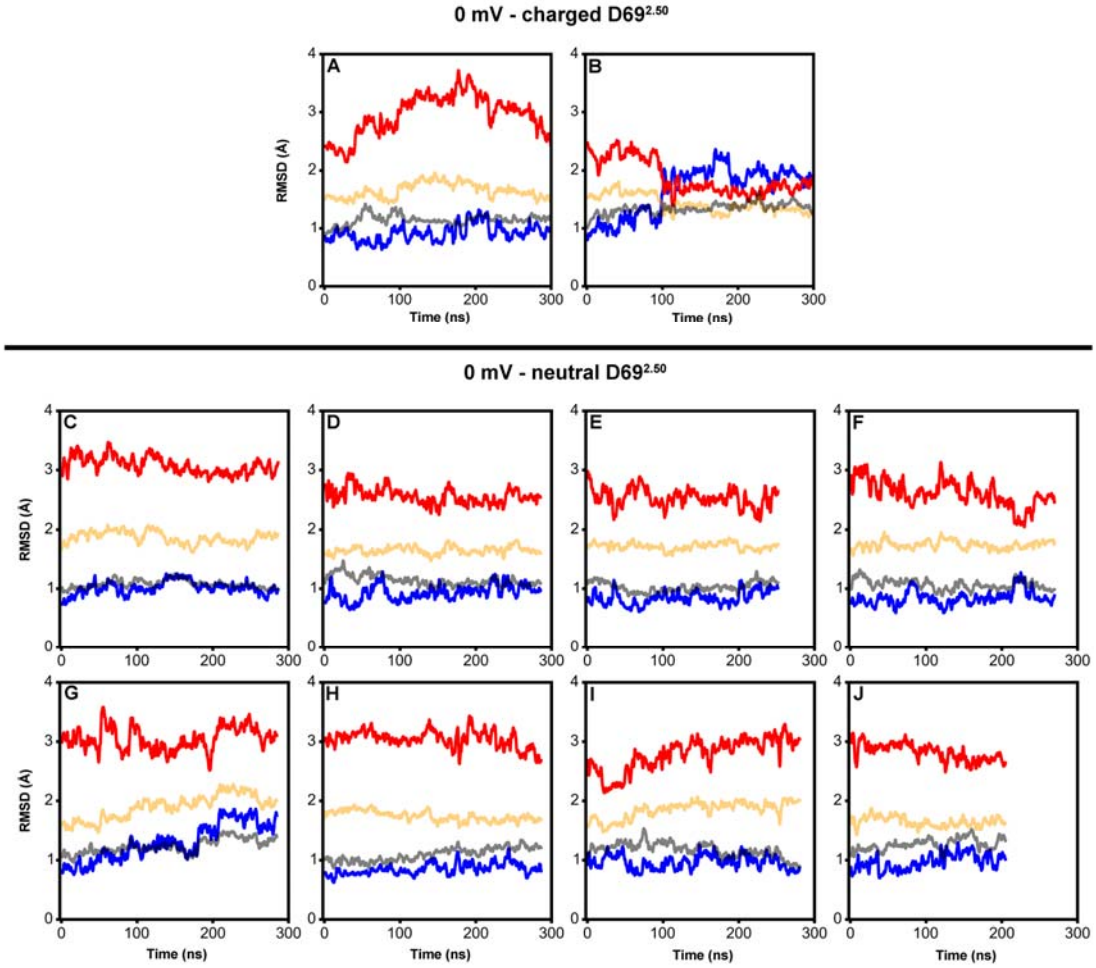

Figure S4: Backbone RMSD values during equilibrium MD simulations (V_m=0) of the active state m2r.

The red and blue lines show RMSD values of helix TM6 with respect to the inactive and active state structures (PDB: 3UON, 4MQT), respectively, while the grey and orange lines show the RMSDs of all TM helices relative to the inactive and active state structures. $D69^{2.50}$ was either charged (A, B) or neutral (C-J). When the Na^+ ion is still bound to $D69^{2.50}$ in simulations with a charged $D69^{2.50}$, the receptor can switch back to the inactive conformation in some trajectories (see panel B; compare grey and orange lines). In contrast, all simulations with a neutral $D69^{2.50}$ remain stable in the active conformation.

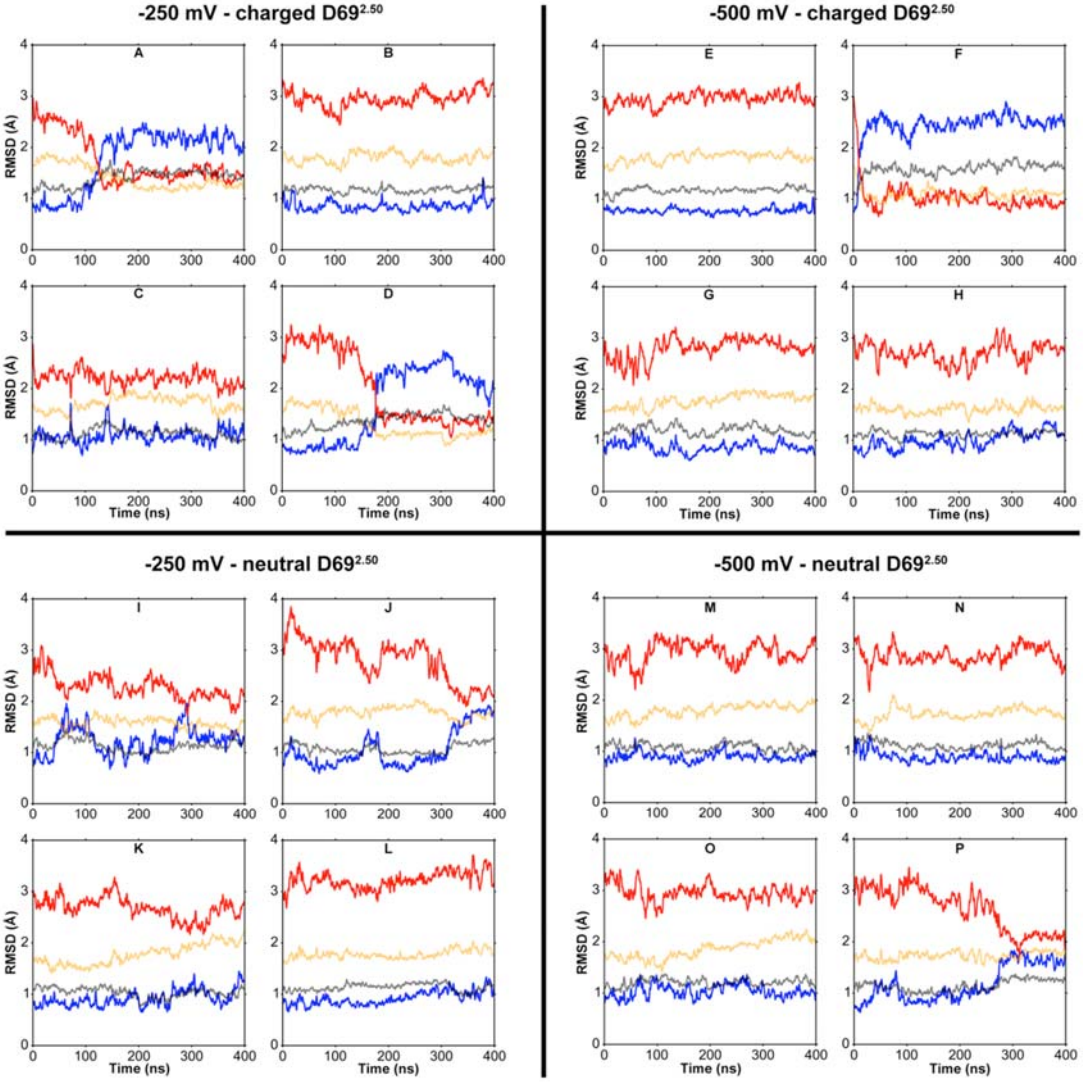

Figure S5: Backbone RMSD values during MD simulations of the active state m2r under membrane voltage.

The red and blue lines show RMSD values of helix TM6 with respect to the inactive and active state structures (PDB: 3UON, 4MQT), respectively, while the grey and orange lines show the RMSDs of all TM helices relative to the inactive and active state structures. The active state simulations were carried out under a V_m of -250mV (A-D, I-L) or -500mV (E-H, M-P), and $D69^{2.50}$ was either charged (A-H) or neutral (I-P). Also see Fig 3 and corresponding discussion in the main text. When the Na^+ ion is still bound to $D69^{2.50}$ in simulations with a charged $D69^{2.50}$, the receptor can switch back to an inactive conformation (e.g. panels A, D and F; compare grey and orange lines). In contrast, most simulations with a neutral $D69^{2.50}$ remain stable in the active state and only two simulations show a change to an intermediate conformation (panels J and P), but no further transitions reverting to the inactive state.

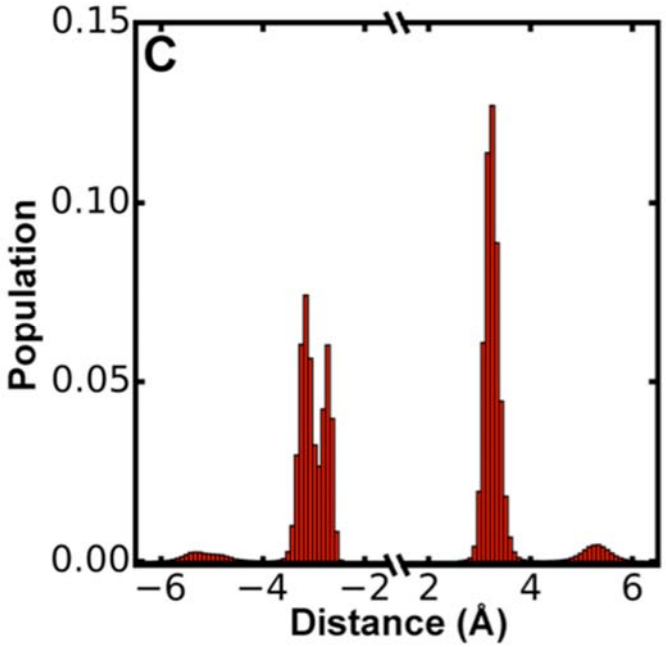

Figure S6: Distribution of distances between the Na^+ ion and $D69^{2.50}$.

Distance distribution between Na^+ and $D69^{2.50}$ (C_γ) in the active state of m2r under -250 mV and charged $D69^{2.50}$. Positive values signify displacements towards the extracellular side, negative values movements towards the intracellular side.

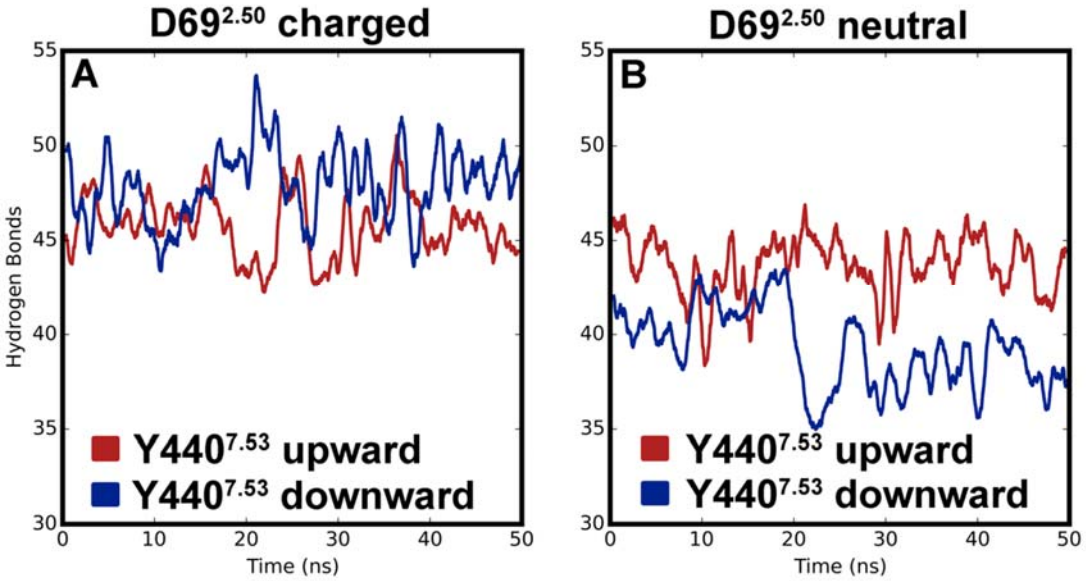

Figure S7: Number of hydrogen bonds around the Na^+ binding site.

The conformation of the $Y440^{7.53}$ sidechain and the protonation state of $D^{2.50}$ affect the number of hydrogen bonds in the hydrophilic region around the Na^+ binding site, defined as lying within 10 Å of the C_γ atom of $D69^{2.50}$. **(A)** With a charged $D69^{2.50}$, a similar number of hydrogen bonds exists, irrespective of the conformation of $Y440^{7.53}$. **(B)** In the case of neutral $D^{2.50}$, the downward conformation of $Y440^{7.53}$ leads to a decrease in the number of hydrogen bonds around the Na^+ binding pocket.

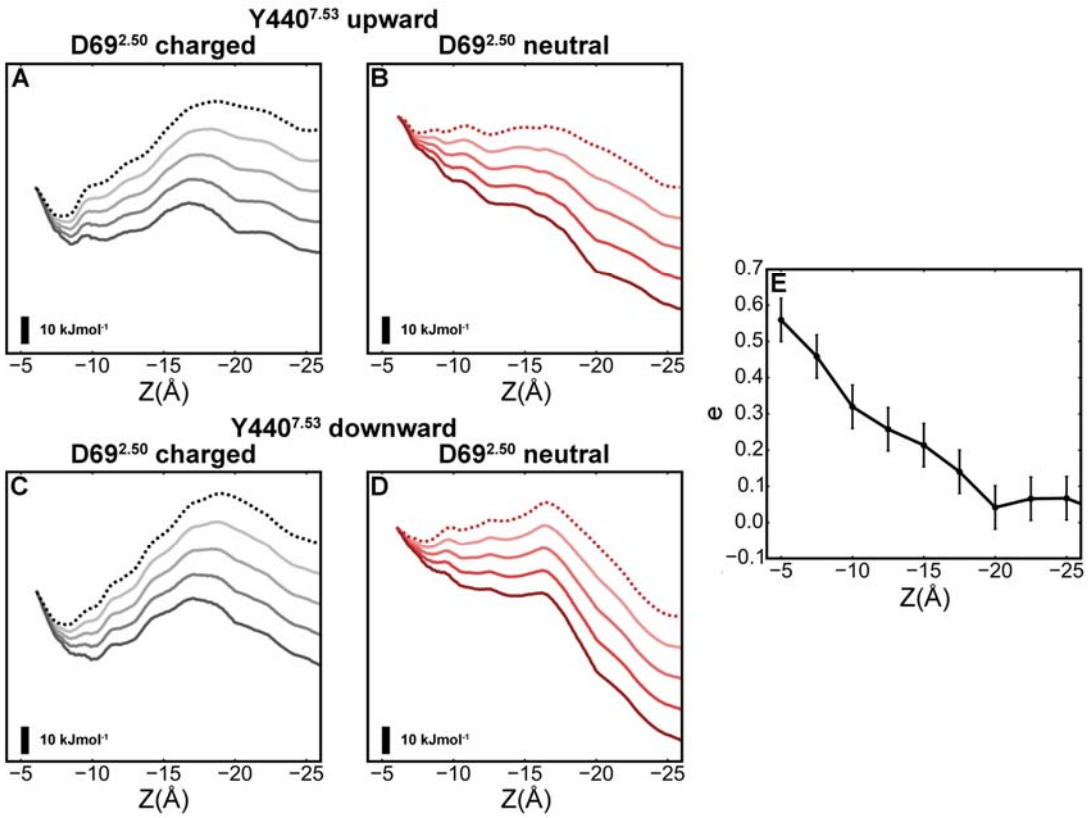

Figure S8: Non-equilibrium effect of V_m upon the PMF profiles of Na^+ translocation to the cytoplasm

(**A**-**D**) Voltage-induced tilt of the free energy profiles (see Fig. 4 in the main text) of Na^+ translocation in m2r in a non-equilibrium case under 4 different conditions: (**A**) $Y440^{7.53}$ upward and $D69^{2.50}$ charged, (**B**) $Y440^{7.53}$ upward and $D69^{2.50}$ neutral, (**C**) $Y440^{7.53}$ downward and $D69^{2.50}$ charged, and (**D**) $Y440^{7.53}$ downward and $D69^{2.50}$ neutral. Increments are from 250 mV (light lines) to 1000 mV (dark lines); a dotted line indicates 0 mV. Similar to the figures in the main text, the Z-coordinate along the vertical axis was calculated relative to the Cα atom of $D103^{3.32}$. The underlying voltage drop was mapped using the calculated gating charge (see below). The panels display the relative free energy differences for each voltage regime; the black bar denotes an energy difference of 10 kJ mol^{-1} within each panel. (**E**) The gating charge, q, was calculated from the simulation of m2r with $Y440^{7.53}$ upward and $D69^{2.50}$ charged (see the Methods section in the main text for details) and is shown in units of the elementary charge *e*.

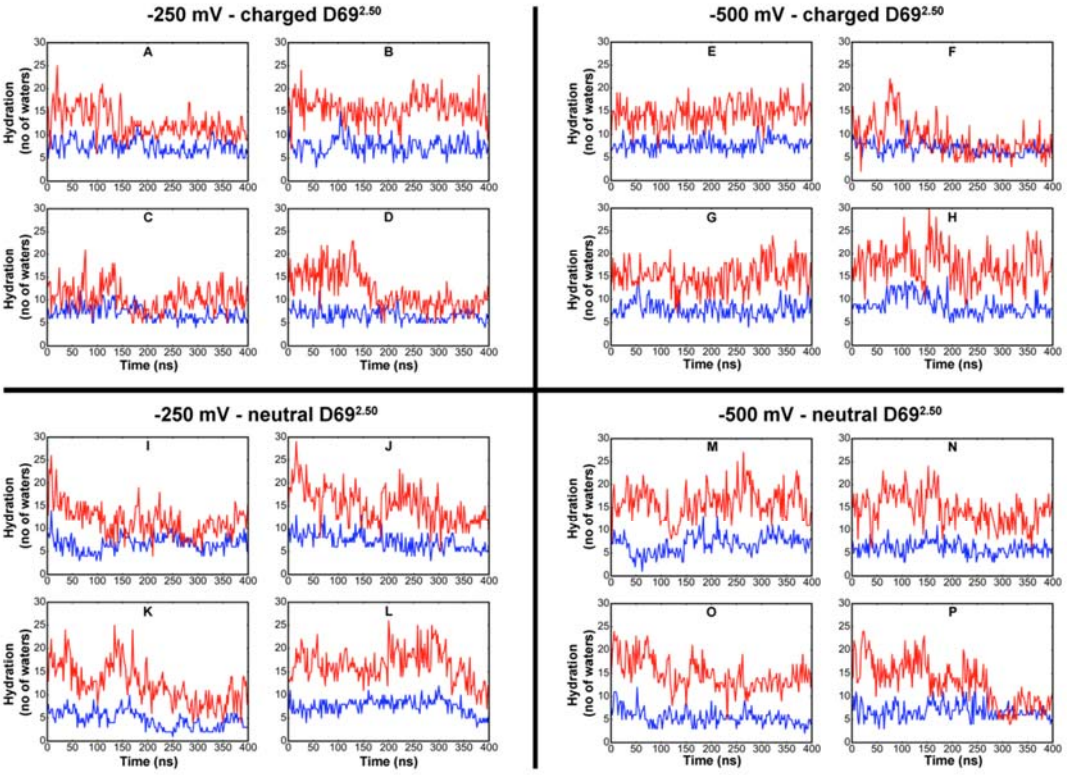

Figure S9: Hydration of the hydrophilic pocket and intracellular effector-binding site.

The hydration level of the m2r receptor is represented by a number of water molecules within two regions: the hydrophilic pocket (blue lines) and the intracellular effector-binding site (red lines). Here we show 4 replicates of each simulation condition: (**A-D**) V_m -250 mV, $D69^{2.50}$ charged, (**E-H**) V_m -500 mV, $D69^{2.50}$ charged, (**I-L**) V_m -250 mV, $D69^{2.50}$ neutral, and (**M-P**) V_m -500 mV, $D69^{2.50}$ neutral. The hydrophilic pocket was defined as Z = ± 4 Å from the $D69^{2.50}$ Cα atom. The channel to the effector-binding site was defined between the Z = -4 Å from the $D69^{2.50}$ Cα atom and the Z-coordinate of the $R121^{3.50}$ Cα. The number of water molecules was recorded every 2 ns throughout the simulations. Also see Table S1 for the mean values.

It can be seen that the number of water molecules within the hydrophilic pocket remains stable throughout all simulations, with a slight decrease when $D69^{2.50}$ is neutral (panels I-P and Table S1). The number of water molecules within the intracellular effector-binding site is stable in the majority of simulations, with a substantial decrease in few cases correlating with the transition of those systems to the inactive or intermediate states (Fig S5 and Table S1).

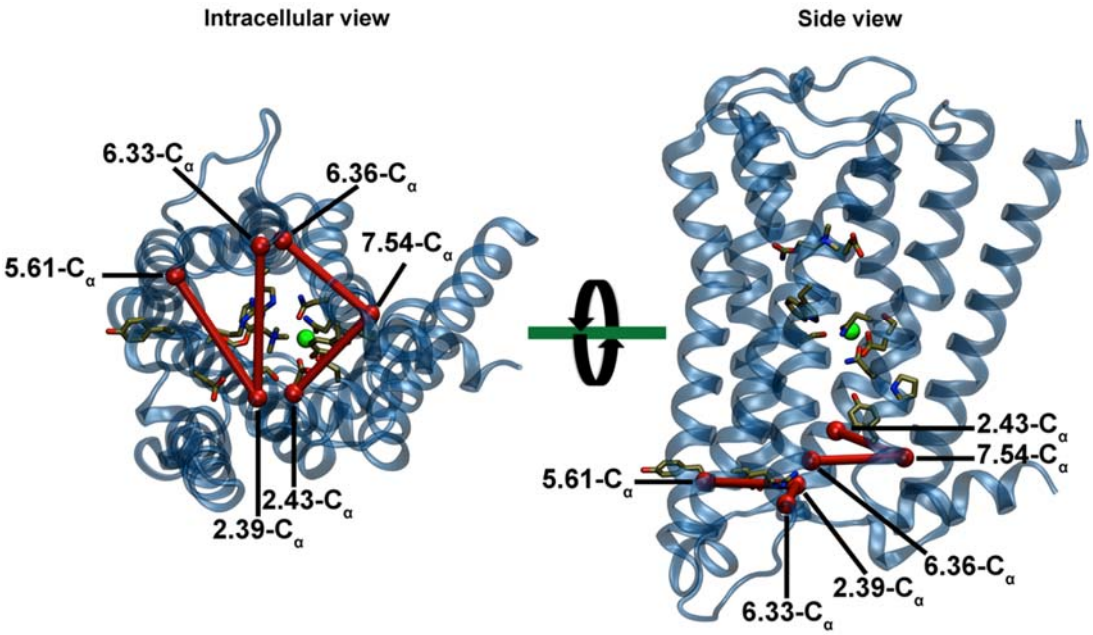

Figure S10: Depiction of the minimal set of distance restraints used to maintain the active conformation of the m2r at the G-protein binding site.

A set of four distance restraints (indicated by red bars) was applied to the intracellular portion of the transmembrane helices as described in the Methods section. This procedure serves to maintain the m2r in the active state despite the absence of a bound G-protein. With the Na^+ ion bound at $D69^{2.50}$, and D2.50 in a charged state, in many simulations without these restraints the receptor regains its inactive conformation on timescales below microseconds, which is in agreement with the role of sodium as stabilizer of the inactive conformation.

$D^{2.50}$ charge state	Transmembrane potential (mV)	Replicate	Na^+ permeation	Hydrophilic pocket hydration	Effector pocket hydration
		1	No	7.6±1.6	12.6±3.1
		2	No	7.5±1.6	15.8±2.7
		3	No	7.2±1.6	10.4±2.9
		4	No	6.7±1.3	12.1±4.1
		1	No	7.9±1.4	14.6±2.6
		2	No	7.0±1.4	9.1±3.7
		3	**Yes**	7.9±1.8	15.2±3.1
		4	No	8.7±2.1	17.5±4.0
		1	**Yes**	6.7±1.7	11.8±3.4
		2	**Yes**	7.2±1.8	15.1±4.0
		3	**Yes**	4.7±1.9	12.2±4.3
		4	No	7.6±1.6	16.4±3.5
		1	**Yes**	6.9±2.0	15.9±3.5
		2	**Yes**	6.0±1.5	14.5±3.5
		3	**Yes**	5.5±1.7	14.8±3.3
		4	**Yes**	6.8±1.7	13.0±4.7

Table S1: Permeation of Na^+ into the cytoplasm and hydration of the m2r receptor.

A list of simulations performed in the presence of V_m detailing the simulation conditions and main observations: TM potential, the charge state of $D69^{2.50}$, observation of Na^+ permeation to the intracellular side, and hydration of the receptor – the number of water molecules (mean ± std) in the hydrophilic pocket (Z = ±4 Å from the $D69^{2.50}$ Cα atom) and in the hydrated channel (between the Z = -4Å from the $D69^{2.50}$ Cα atom and the Z-coordinate of the $R121^{3.50}$ Cα). For each condition four independent replicates were simulated for 400 ns. The number of water molecules was recorded every 2 ns throughout the simulations. Also see Fig S9.

Residue	Consensus among muscarinic receptors	Consensus among aminergic receptor	Consensus among class A GPCRs
N41$^{1.50}$	N (100%)	N (100%)	N (98%)
N58$^{2.39}$	N (100%)	T (47%), Polar (81%)	T (37%), Polar (54%)
N59$^{2.40}$	N (100%)	N (92%)	N (39%), Polar (73%)
L62$^{2.43}$	L (100%)	I (50%), Hydrophobic (100%)	L (36%), Hydrophobic (96%)
L65$^{2.46}$	L (100%)	L (94%)	L (90%)
A66$^{2.47}$	A (100%)	A (94%)	A (73%)
A68$^{2.49}$	A (100%)	A (64%)	A (56%)
D69$^{2.50}$	D (100%)	D (100%)	D (92%)
I72$^{2.53}$	I (100%)	V (58%), Hydrophobic (100%)	V (23%), Hydrophobic (88%)
V106$^{3.35}$	A (60%), V (40%)	C (44%), Hydrophobic (100%)	N (26%), Hydrophobic (39%)
S107$^{3.36}$	S (100%)	C (56%)	M (19%)
A109$^{3.38}$	A (100%)	A (81%)	A (38%)
S110$^{3.39}$	S (100%)	S (100%)	S (72%)
V111$^{3.40}$	V (100%)	I (81%), Hydrophobic (100%)	I (38%), Hydrophobic (89%)
L114$^{3.43}$	L (100%)	L (89%)	L (73%)
I117$^{3.46}$	I (100%)	I (94%)	I (56%)
D120$^{3.49}$	D (100%)	D (100%)	D (64%)
R121$^{3.50}$	R (100%)	R (100%)	R (94%)
C124$^{3.53}$	S (60%), C (40%)	A (56%), Hydrophobic (64%)	A (47%), Hydrophobic (68%)
Y206$^{5.58}$	Y (100%)	Y (94%)	Y (73%)
V385$^{6.33}$	A (60%), V (40%)	A (72%), Hydrophobic (97%)	A (29%)
T388$^{6.36}$	T (100%)	T (58%)	T (25%)
I392$^{6.40}$	I (100%)	I (53%), Hydrophobic (100%)	V (47%), Hydrophobic (100%)
A395$^{6.43}$	A (100%)	A (39%)	V (31%)
F396$^{6.44}$	F (100%)	F (100%)	F (75%)
T399$^{6.47}$	T (100%)	C (72%)	C (70%)
W400$^{6.48}$	W (100%)	W (100%)	W (68%)
N432$^{7.45}$	N (100%)	N (92%)	N (67%)
S433$^{7.46}$	S (100%)	S (100%)	S (64%)
T434$^{7.47}$	T (100%)	A/T (22%)	C (39%)
I435$^{7.48}$	I (60%), V (40%)	L (33%), Hydrophobic (100%)	L (34%), Hydrophobic (96%)
N436$^{7.49}$	N (100%)	N (100%)	N (71%)
P437$^{7.50}$	P (100%)	P (100%)	P (93%)
C439$^{7.52}$	C (100%)	I (61%), Hydrophobic (100%)	I (41%), Hydrophobic (99%)
Y440$^{7.53}$	Y (100%)	Y (100%)	Y (89%)
C443$^{7.56}$	C (100%)	F (44%)	L (23%)

Table S2. Conservation of the residues in the transmembrane region that were observed to be in contact (>4.5 Å) with Na^+ in the MD simulations. Overall, the sodium ion was observed to come into close proximity with 34 residues.